Pseudogaps in strongly correlated metals: Optical conductivity within the generalized dynamical mean-field theory approach

E. Z. Kuchinskii, I. A. Nekrasov, and M. V. Sadovskii
Institute for Electrophysics, Russian Academy of Sciences, Ekaterinburg 620016, Russia
(Received 19 September 2006; revised manuscript received 24 October 2006; published 5 March 2007)

The optical conductivity of the weakly doped two-dimensional repulsive Hubbard model on the square lattice with the nearest and next-nearest hoppings is calculated within the generalized dynamical mean-field (DMFT+$\Sigma_{\mathbf{p}}$) approach, which includes correlation length scale ξ into the standard DMFT equations via the momentum dependent self-energy $\Sigma_{\mathbf{p}}$, with a full account of appropriate vertex corrections. This approach takes into consideration the nonlocal dynamical correlations induced, e.g., by short-ranged collective spin-density-wavelike antiferromagnetic spin fluctuations, which (at high enough temperatures) can be viewed as a quenched Gaussian random field with finite correlation length ξ. The DMFT effective single-impurity problem is solved by numerical renormalization group. We consider both the case of correlated metal with the bandwidth $W \lesssim U$ and that of doped Mott insulator with $U \gg W$ (U—the value of local Hubbard interaction). The optical conductivity calculated within DMFT+$\Sigma_{\mathbf{p}}$ demonstrates typical pseudogap behavior within the quasiparticle band, in qualitative agreement with experiments in copper oxide superconductors. For large values of U, pseudogap anomalies are effectively suppressed.

DOI: 10.1103/PhysRevB.75.115102 PACS number(s): 71.10.Fd, 71.10.Hf, 71.27.+a, 71.30.+h

I. INTRODUCTION

Pseudogap state is a major anomaly of the electronic properties of underdoped copper oxides[1,2]. We believe that the preferable "scenario" for its formation is most likely based on the model of strong scattering of electrons by short-ranged antiferromagnetic (AFM), spin-density-wave (SDW) spin fluctuations.[2] This scattering mainly transfers momenta of the order of $\mathbf{Q}=\left(\frac{\pi}{a},\frac{\pi}{a}\right)$ (a—the lattice constant of a two-dimensional lattice), leading to the formation of structures in the one-particle spectrum, which are precursors of the changes in the spectra due to long-range AFM order (period doubling) with non-Fermi-liquid-like behavior of the spectral density in the vicinity of the so-called hot spots on the Fermi surface, appearing at the intersections of the Fermi surface with antiferromagnetic Brillouin-zone boundary (umklapp surface).[2]

In recent years, a simplified model of the pseudogap state was studied[2–4] under the assumption that the scattering by dynamic spin fluctuations can be reduced for high enough temperatures to a static Gaussian random field (quenched disorder) of pseudogap fluctuations. These fluctuations are defined by characteristic scattering vectors of the order of $\mathbf{Q}$, with distribution width determined by the inverse correlation length of short-range order $\kappa=\xi^{-1}$ and by appropriate energy scale Δ (typically of the order of the crossover temperature T^* to the pseudogap state[2]).

It is also well known that undoped cuprates are antiferromagnetic Mott insulators with $U \gg W$ (U—the value of the local Hubbard interaction, W—the bandwidth of noninteracting band), so that correlation effects are very important and underdoped (and probably also optimally doped) cuprates are actually typical strongly correlated metals.

The cornerstone of the modern theory of strongly correlated systems is the dynamical mean-field theory (DMFT).[5–9] At the same time, standard DMFT is not appropriate for the "antiferromagnetic" scenario of pseudogap formation in strongly correlated metals due to the basic approximation of the DMFT, which completely neglects nonlocal dynamical correlation effects.

Different extensions of DMFT were proposed in recent years to cure this deficiency, such as extended DMFT (EDMFT),[10,11] which locally includes coupling to nonlocal dynamical fluctuations, and, most importantly, different versions of the so-called cluster mean-field theories, such as the dynamical cluster approximation[12] and cellular DMFT.[13] However, these approaches have certain drawbacks. First of all, the effective quantum single impurity problem becomes rather complex. Thus, majority of computational tools available for the DMFT can be used only for small enough clusters,[12] which include mostly nearest-neighbor fluctuations. It is especially difficult to apply these methods to the calculations of two-particle properties, e.g., optical conductivity.

Recently, we have proposed a generalized DMFT+$\Sigma_{\mathbf{p}}$ approach.[14–16] This approach, on the one hand, retains the single-impurity description of the DMFT, which properly accounts for *local* correlations, and the possibility to use impurity solvers such as numerical renormalization group (NRG).[25,26] On the other hand, this approach includes nonlocal correlations on a nonperturbative model basis, which allows us to control the characteristic scales and also the types of nonlocal fluctuations. This latter point allows us to systematically study the influence of nonlocal fluctuations on the electronic properties and, in particular, provides valuable hints on the physical origin and possible interpretation of the results. Within this approach, we have studied single-particle properties, such as pseudogap formation in the density of states of the quasiparticle band for both correlated metal and doped Mott insulator, evolution of the non-Fermi-liquid-like spectral density and angle-resolved photoemission spectra,[15] "destruction" of Fermi surfaces and formation of Fermi "arcs,"[14] as well as impurity scattering effects.[16] This formalism was also combined with modern local-density approxi-

mation (LDA)+DMFT calculations of the electronic structure of "realistic" correlated systems to formulate the LDA +DMFT+$\Sigma_{\mathbf{p}}$ approach, which was applied for the description of pseudogap behavior in $Bi_2Ca_2SrCu_2O_8$.[17]

In this paper, we develop our DMFT+$\Sigma_{\mathbf{p}}$ approach for the calculations of two-particle properties, such as (dynamic) optical conductivity, which is conveniently calculated within the standard DMFT.[7,8] We show that inclusion of nonlocal correlations (pseudogap fluctuations) with characteristic length scale ξ allows us to describe the pseudogap effects in longitudinal conductivity of the two-dimensional Hubbard plane.

The paper is organized as follows. In Sec. II we present a short description of our DMFT+$\Sigma_{\mathbf{p}}$ approach. In Sec. III we derive the basic DMFT+$\Sigma_{\mathbf{p}}$ expressions for dynamic (optical) conductivity, as well as formulate recurrence equations to calculate the **p**-dependent self-energy and appropriate vertex part, which take into account all the relevant Feynaman digrams of perturnbation series over pseudogap fluctuations. The computational details and basic results for optical conductivity are given in Sec. IV. We also compare our results with that of the standard DMFT. The paper ends with a summary, Sec. V, including a short overview of related experimental results.

II. BASICS OF THE DMFT+$\Sigma_{\mathbf{p}}$ APPROACH

As noted above, the basic shortcoming of the traditional DMFT approach[5–9] is the neglect of momentum dependence of the electron self-energy. To include nonlocal effects while remaining within the usual "single-impurity analogy," we have proposed[14–16] the following (DMFT+$\Sigma_{\mathbf{p}}$) approach. First of all, the Matsubara "time" Fourier-transformed single-particle Green's function of the Hubbard model is written in obvious notations as

$$G(i\varepsilon,\mathbf{p}) = \frac{1}{i\varepsilon + \mu - \varepsilon(\mathbf{p}) - \Sigma(i\varepsilon) - \Sigma_{\mathbf{p}}(i\varepsilon)},$$

$$\varepsilon = \pi T(2n+1), \tag{1}$$

where $\Sigma(i\varepsilon)$ is the local contribution to the self-energy of DMFT type (surviving in the limit of spatial dimensionality $d \to \infty$) while $\Sigma_{\mathbf{p}}(i\varepsilon)$ is some momentum dependent part. This last contribution can be due either to electron interactions with some "additional" collective modes or to order parameter fluctuations or may be induced by similar nonlocal contributions within the Hubbard model itself. No double-counting problem arises in this approach, as discussed in detail in Ref. 15. At the same time, our procedure does not represent any systematic $1/d$ expansion, as stressed in Refs. 14–16. The basic assumption here is the neglect of all interference processes of the local Hubbard interaction and nonlocal contributions owing to these additional scatterings (noncrossing approximation for appropriate diagrams),[15] as illustrated by the diagrams in Fig. 1.

The self-consistency equations of the generalized DMFT +$\Sigma_{\mathbf{p}}$ approach are formulated as follows:[14,15]

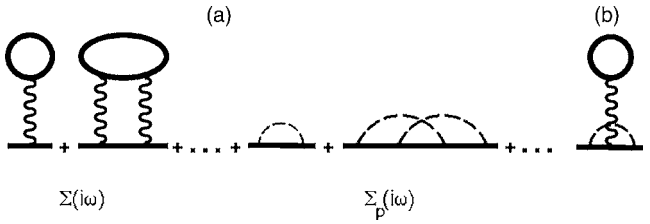

FIG. 1. Typical "skeleton" diagrams for the self-energy in the DMFT+$\Sigma_{\mathbf{p}}$ approach. The first two terms are examples of the DMFT self-energy diagrams, the middle two diagrams show some contributions to the nonlocal part of the self-energy (e.g., from spin fluctuations) represented as dashed lines, and the last diagram (b) is an example of the neglected diagrams leading to interference between the local and nonlocal parts.

(1) Start with some initial guess of local self-energy $\Sigma(i\varepsilon)$, e.g., $\Sigma(i\varepsilon)=0$.

(2) Construct $\Sigma_{\mathbf{p}}(i\varepsilon)$ within some (approximate) scheme, taking into account the interactions with collective modes or order parameter fluctuations, which, in general, can depend on $\Sigma(i\omega)$ and μ.

(3) Calculate the local Green's function,

$$G_{ii}(i\varepsilon) = \frac{1}{N}\sum_{\mathbf{p}} \frac{1}{i\varepsilon + \mu - \varepsilon(\mathbf{p}) - \Sigma(i\varepsilon) - \Sigma_{\mathbf{p}}(i\varepsilon)}. \tag{2}$$

(4) Define the "Weiss field"

$$\mathcal{G}_0^{-1}(i\varepsilon) = \Sigma(i\varepsilon) + G_{ii}^{-1}(i\varepsilon). \tag{3}$$

(5) Using some "impurity solver," calculate the single-particle Green's function $G_d(i\varepsilon)$ for the effective Anderson impurity problem, placed at lattice site i and defined by the effective action which is written, in obvious notations, as

$$S_{\text{eff}} = -\int_0^\beta d\tau_1 \int_0^\beta d\tau_2\, c_{i\sigma}(\tau_1)\mathcal{G}_0^{-1}(\tau_1-\tau_2)c_{i\sigma}^+(\tau_2) + \int_0^\beta d\tau\, U n_{i\uparrow}(\tau)n_{i\downarrow}(\tau). \tag{4}$$

(6) Define a *new* local self-energy,

$$\Sigma(i\omega) = \mathcal{G}_0^{-1}(i\omega) - G_d^{-1}(i\omega). \tag{5}$$

(7) Using this self-energy as the "initial" one in step (1), continue the procedure until (and if) convergency is reached to obtain

$$G_{ii}(i\varepsilon) = G_d(i\varepsilon). \tag{6}$$

Eventually, we get the desired Green's function in the form of Eq. (1), where $\Sigma(i\varepsilon)$ and $\Sigma_{\mathbf{p}}(i\varepsilon)$ are those appearing at the end of our iteration procedure.

III. OPTICAL CONDUCTIVITY IN DMFT+$\Sigma_{\mathbf{p}}$

A. Basic expressions for optical conductivity

To calculate dynamic conductivity, we use the general expression relating it to the retarded density-density correlation function $\chi^R(\omega,\mathbf{q})$ as follows:[18,19]

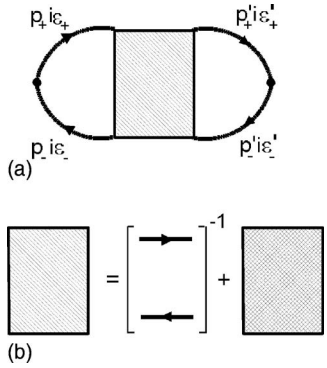

FIG. 2. Full polarization loop (a) with vertex part, which includes free-electron contribution in addition to the standard vertex, containing all interactions (b). Here, $\mathbf{p}_\pm = \mathbf{p} \pm \frac{\mathbf{q}}{2}$ and $\varepsilon_\pm = \varepsilon \pm \frac{\omega}{2}$.

$$\sigma(\omega) = -\lim_{q\to 0} \frac{ie^2\omega}{q^2}\chi^R(\omega,\mathbf{q}), \tag{7}$$

where e is the electronic charge.

Consider the full polarization loop graph in the Matsubara representation, as shown in Fig. 2(a), which is conveniently (with explicit frequency summation) written as

$$\Phi(i\omega,\mathbf{q}) = \sum_{\varepsilon\varepsilon'} \Phi_{i\varepsilon i\varepsilon'}(i\omega,\mathbf{q}) \equiv \sum_{\varepsilon} \Phi_{i\varepsilon}(i\omega,\mathbf{q}), \tag{8}$$

and contains all possible interactions of our model, described by the full vertex part of Fig. 2(b). Note that we use a slightly unusual definition of the vertex part to include the loop contribution without vertex corrections, which shortens further diagrammatic expressions. Retarded density-density correlation function is determined by appropriate analytic continuation of this loop and can be written as

$$\chi^R(\omega,\mathbf{q}) = \int_{-\infty}^{\infty} \frac{d\varepsilon}{2\pi i}\{[f(\varepsilon_+) - f(\varepsilon_-)]\Phi_\varepsilon^{RA}(\mathbf{q},\omega) + f(\varepsilon_-)\Phi_\varepsilon^{RR}(\mathbf{q},\omega) - f(\varepsilon_+)\Phi_\varepsilon^{AA}(\mathbf{q},\omega)\}, \tag{9}$$

where $f(\varepsilon)$ is the Fermi distribution, $\varepsilon_\pm = \varepsilon \pm \frac{\omega}{2}$, and the two-particle loops $\Phi_\varepsilon^{RA}(\mathbf{q},\omega)$, $\Phi_\varepsilon^{RR}(\mathbf{q},\omega)$, $\Phi_\varepsilon^{AA}(\mathbf{q},\omega)$ are determined by appropriate analytic continuations ($i\varepsilon + i\omega \to \varepsilon + \omega + i\delta$, $i\varepsilon \to \varepsilon \pm i\delta$, and $\delta \to +0$) in Eq. (8). Then we can conveniently write the dynamic conductivity as

$$\sigma(\omega) = \lim_{q\to 0}\left(-\frac{e^2\omega}{2\pi q^2}\right)\int_{-\infty}^{\infty} d\varepsilon\{[f(\varepsilon_+) - f(\varepsilon_-)][\Phi_\varepsilon^{RA}(\mathbf{q},\omega) - \Phi_\varepsilon^{RA}(0,\omega)] + f(\varepsilon_-)[\Phi_\varepsilon^{RR}(\mathbf{q},\omega) - \Phi_\varepsilon^{RR}(0,\omega)] - f(\varepsilon_+) \times [\Phi_\varepsilon^{AA}(\mathbf{q},\omega) - \Phi_\varepsilon^{AA}(0,\omega)]\}, \tag{10}$$

where the total contribution of the additional terms with zero q can be shown (with the use of the general Ward identities[20]) to be zero.

To calculate $\Phi_{i\varepsilon i\varepsilon'}(i\omega,\mathbf{q})$ entering the sum over the Matsubara frequencies in Eq. (8) in the DMFT+$\Sigma_\mathbf{p}$ approximation, which neglects the interference between local Hubbard

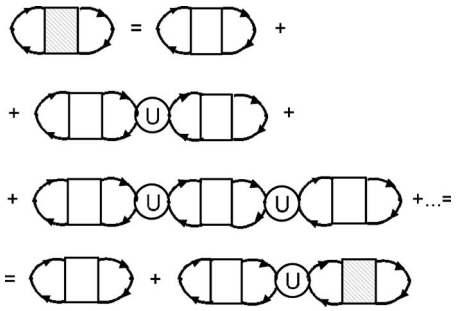

FIG. 3. Bethe-Salpeter equation for the polarization loop in the DMFT+$\Sigma_\mathbf{p}$ approach. The circles represent irreducible vertex part of DMFT, which contains only local interactions, surviving in the limit of $d\to\infty$. The unshaded rectangular vertex represents nonlocal interactions, e.g., with SDW (pseudogap) fluctuations, which is similarly defined to Fig. 2(b).

interaction and nonlocal contributions due to additional scatterings, e.g., by SDW pseudogap fluctuations,[15] we can write down the Bethe-Salpeter equation, as shown diagrammatically in Fig. 3, where we have introduced the irreducible (local) vertex $U_{i\varepsilon i\varepsilon'}(i\omega)$ of DMFT and "rectangular" vertex, defined as in Fig. 2(b) and containing all interactions with fluctuations. Analytically, this equation can be written as

$$\Phi_{i\varepsilon i\varepsilon'}(i\omega,\mathbf{q}) = \Phi^0_{i\varepsilon}(i\omega,\mathbf{q})\delta_{\varepsilon\varepsilon'} + \Phi^0_{i\varepsilon}(i\omega,\mathbf{q})\sum_{\varepsilon''} U_{i\varepsilon i\varepsilon''}(i\omega)\Phi_{i\varepsilon'' i\varepsilon'}(i\omega,\mathbf{q}), \tag{11}$$

where $\Phi^0_{i\varepsilon}(i\omega,\mathbf{q})$ is the desired function calculated neglecting vertex corrections due to the Hubbard interaction (but taking into account all nonlocal interactions with fluctuations considered here to be static). Note that all q dependence here is determined by $\Phi^0_{i\varepsilon}(i\omega,\mathbf{q})$, as the vertex $U_{i\varepsilon i\varepsilon'}(i\omega)$ is local and q independent.

As clearly seen from Eq. (10), to calculate the conductivity, we need only to find the q^2 contribution to $\Phi(i\omega,\mathbf{q})$ defined in Eq. (8). This can be done in the following way. First of all, note that all the loops in Eq. (11) contain the q dependence starting from terms of the order of q^2. Then, we can take an arbitrary loop (cross section) in the expansion of Eq. (11) (see Fig. 3), calculating it up to terms of the order of q^2, and make a resummation of all the contributions to the right and to the left of this cross section (using the obvious left-right symmetry of diagram summation in the Bethe-Salpeter equation), putting $\mathbf{q}=0$ in all these graphs. This is equivalent to the simple q^2 differentiation of the expanded version of Eq. (11). This procedure immediately leads to the following relation for q^2 contribution to Eq. (8):

$$\phi(i\omega) \equiv \lim_{q\to 0}\frac{\Phi(i\omega,\mathbf{q}) - \Phi(i\omega,0)}{q^2} = \sum_{\varepsilon} \gamma^2_{i\varepsilon}(i\omega,\mathbf{q}=0)\phi^0_{i\varepsilon}(i\omega), \tag{12}$$

where

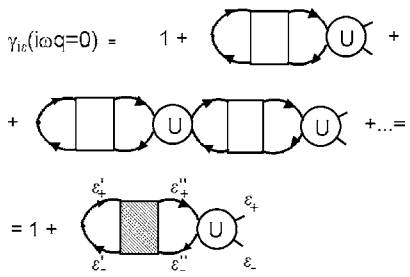

FIG. 4. Effective vertex $\gamma_{i\varepsilon}(i\omega,\mathbf{q}=0)$ used in the calculations of conductivity.

$$\phi^0_{i\varepsilon}(i\omega) \equiv \lim_{q\to 0} \frac{\Phi^0_{i\varepsilon}(i\omega,\mathbf{q}) - \Phi^0_{i\varepsilon}(i\omega,0)}{q^2}, \tag{13}$$

with $\Phi^0_{i\varepsilon}(i\omega,\mathbf{q})$ containing the vertex corrections only due to nonlocal (pseudogap) fluctuations, while the one-particle Green's functions in it are taken with self-energies due to both these fluctuations and local DMFT-like interaction, as in Eq. (1). The vertex $\gamma_{i\varepsilon}(i\omega,\mathbf{q}=0)$ is determined diagrammatically as shown in Fig. 4, or analytically,

$$\gamma_{i\varepsilon}(i\omega,\mathbf{q}=0) = 1 + \sum_{\varepsilon'\varepsilon''} U_{i\varepsilon i\varepsilon''}(i\omega)\Phi_{i\varepsilon'' i\varepsilon'}(i\omega,\mathbf{q}=0). \tag{14}$$

Now, using the Bethe-Salpeter equation (11), we can explicitly write

$$\gamma_{i\varepsilon}(i\omega,\mathbf{q}=0) = 1 + \sum_{\varepsilon'} \frac{\Phi_{i\varepsilon i\varepsilon'}(i\omega,\mathbf{q}=0) - \Phi^0_{i\varepsilon}(i\omega,\mathbf{q}=0)}{\Phi^0_{i\varepsilon}(i\omega,\mathbf{q}=0)} = \frac{\sum_{\varepsilon'} \Phi_{i\varepsilon i\varepsilon'}(i\omega,\mathbf{q}=0)}{\Phi^0_{i\varepsilon}(i\omega,\mathbf{q}=0)}. \tag{15}$$

For $\mathbf{q}=0$, we have the following Ward identity, which can be obtained by a direct generalization of the proof given in Refs. 18 and 20 (see the Appendix):

$$(-i\omega)\Phi_{i\varepsilon}(i\omega,\mathbf{q}=0) = (-i\omega)\sum_{\varepsilon'} \Phi_{i\varepsilon i\varepsilon'}(i\omega,\mathbf{q}=0) = \sum_{\mathbf{p}} G(i\varepsilon+i\omega,\mathbf{p}) - \sum_{\mathbf{p}} G(i\varepsilon,\mathbf{p}). \tag{16}$$

The denominator of Eq. (15) contains vertex corrections only from nonlocal correlations (e.g., pseudogap fluctuations), while Green's functions here are "dressed" *both* by these correlations and the local (DMFT) Hubbard interaction. Thus, we may consider the loop entering the denominator as dressed by (pseudogap) fluctuations only, but with "bare" Green's functions:

$$\tilde{G}_0(i\varepsilon,\mathbf{p}) = \frac{1}{i\varepsilon + \mu - \varepsilon(\mathbf{p}) - \Sigma(i\varepsilon)}, \tag{17}$$

where $\Sigma(i\varepsilon)$ is the local contribution to the self-energy from DMFT. For this problem, we have the following Ward identity, similar to Eq. (16) (see the Appendix):

$$\sum_{\mathbf{p}} G(i\varepsilon+i\omega,\mathbf{p}) - \sum_{\mathbf{p}} G(i\varepsilon,\mathbf{p}) = \Phi^0_{i\varepsilon}(i\omega,\mathbf{q}=0)\left[\Sigma(i\varepsilon+i\omega) - \Sigma(i\varepsilon) - i\omega\right] \equiv \Phi^0_{i\varepsilon}(i\omega,\mathbf{q}=0)\left[\Delta\Sigma(i\omega) - i\omega\right], \tag{18}$$

where we have introduced

$$\Delta\Sigma(i\omega) = \Sigma(i\varepsilon+i\omega) - \Sigma(i\varepsilon). \tag{19}$$

Thus, using Eqs. (16) and (18) in Eq. (15), we get the final expression for $\gamma_{i\varepsilon}(i\omega,\mathbf{q}=0)$ as follows:

$$\gamma_{i\varepsilon}(i\omega,\mathbf{q}=0) = 1 - \frac{\Delta\Sigma(i\omega)}{i\omega}. \tag{20}$$

Then, Eq. (12) reduces to

$$\phi(i\omega) = \sum_{\varepsilon} \phi^0_{i\varepsilon}(i\omega)\left[1 - \frac{\Delta\Sigma(i\omega)}{i\omega}\right]^2. \tag{21}$$

The analytic continuation to real frequencies is obvious, and using Eqs. (12) and (21) in Eq. (10), we can write the final expression for the real part of dynamic conductivity as

$$\mathrm{Re}\,\sigma(\omega) = \frac{e^2\omega}{2\pi}\int_{-\infty}^{\infty} d\varepsilon[f(\varepsilon_-) - f(\varepsilon_+)]\mathrm{Re} \times \left\{ \phi^{0RA}_{\varepsilon}(\omega)\left[1 - \frac{\Sigma^R(\varepsilon_+) - \Sigma^A(\varepsilon_-)}{\omega}\right]^2 - \phi^{0RR}_{\varepsilon}(\omega)\left[1 - \frac{\Sigma^R(\varepsilon_+) - \Sigma^R(\varepsilon_-)}{\omega}\right]^2 \right\}. \tag{22}$$

Thus we have achieved a great simplification of our problem. To calculate the optical conductivity in DMFT+$\Sigma_{\mathbf{p}}$, we only have to solve the single-particle problem as described by the DMFT+$\Sigma_{\mathbf{p}}$ procedure above to determine the self-consistent values of the local self-energies $\Sigma(\varepsilon_\pm)$, while the nontrivial contribution of nonlocal correlations is to be included via Eq. (13), which is to be calculated in some approximation, taking into account only the interaction with nonlocal (e.g., pseudogap) fluctuations, but using the bare Green's functions of the form Eq. (17), which include local self-energies already determined in the general DMFT+$\Sigma_{\mathbf{p}}$ procedure. Actually, Eq. (22) also provides an effective algorithm to calculate the dynamic conductivity in standard DMFT (neglecting any nonlocal correlations), as Eq. (13) is then easily calculated from a simple loop diagram, determined by two Green's functions and free *scalar* vertices. As usual, there is no need to calculate the vertex corrections within the DMFT itself, as was proven first by considering the loop with *vector* vertices.[7,8]

B. Recurrence relations for self-energy and vertex parts

As we are mainly interested in the pseudogap state of copper oxides, we shall further concentrate on the effects of scattering of electrons from collective short-range SDW-like antiferromagnetic spin fluctuations. In a kind of simplified approach, valid only for high enough temperatures,[3,4] we shall calculate $\Sigma_{\mathbf{p}}(i\omega)$ for an electron moving in the quenched random field of (static) Gaussian spin fluctuations, with dominant scattering momentum transfers from the vicinity of some characteristic vector $\mathbf{Q}$ (hot-spot model[2]), using (as we have done in Refs. 14–16) a slightly generalized version of the recurrence procedure proposed in Refs. 3, 4, and 21 (see also Ref. 19), which takes into account *all* Feynman diagrams describing the scattering of electrons by this random field. In general, the neglect of fluctuation dynamics overestimates pseudogap effects. Referring the reader to earlier papers for details,[3,4,14–16] here we just start with the main recurrence relation determining the self-energy as follows:

$$\Sigma_k(i\varepsilon,\mathbf{p}) = \Delta^2 \frac{s(k)}{i\varepsilon + \mu - \Sigma(i\varepsilon) - \varepsilon_k(\mathbf{p}) + inv_k\kappa - \Sigma_{k+1}(i\varepsilon,\mathbf{p})}. \tag{23}$$

Usually, one takes the value of Σ_{k+1} for large enough k equal to zero, and doing the recurrence backwards to $k=1$, we get the desired physical self-energy $\Sigma(i\varepsilon,\mathbf{p})=\Sigma_1(i\varepsilon,\mathbf{p})$.[4,19,21]

In Eq. (23), Δ characterizes the energy scale and $\kappa=\xi^{-1}$ is the inverse correlation length of short-range SDW fluctuations; $\varepsilon_k(\mathbf{p})=\varepsilon(\mathbf{p}+\mathbf{Q})$ and $v_k=|v^x_{\mathbf{p}+\mathbf{Q}}|+|v^y_{\mathbf{p}+\mathbf{Q}}|$ for odd k while $\varepsilon_k(\mathbf{p})=\varepsilon(\mathbf{p})$ and $v_k=|v^x_{\mathbf{p}}|+|v^y_{\mathbf{p}}|$ for even k. The velocity projections $v^x_{\mathbf{p}}$ and $v^y_{\mathbf{p}}$ are determined by the usual momentum derivatives of the bare electronic energy dispersion $\varepsilon(\mathbf{p})$. Finally, $s(k)$ represents a combinatorial factor, which is always assumed here to be that corresponding to the case of Heisenberg spin fluctuations in the "nearly antiferromagnetic Fermi liquid" (spin-fermion model of Ref. 3, SDW-type fluctuations):

$$s(k) = \begin{cases} \dfrac{k+2}{3} & \text{for odd } k, \\ \dfrac{k}{3} & \text{for even } k. \end{cases} \tag{24}$$

As was stressed in Refs. 15 and 16 this procedure introduces an important length scale ξ not present in standard DMFT, which mimics the effect of short-range (SDW) correlations within fermionic "bath" surrounding the DMFT effective single Anderson impurity.

An important aspect of the theory is that both parameters Δ and ξ can, in principle, be calculated from the microscopic model at hand,[15] but here we consider these as phenomenological parameters of the theory (i.e., to be determined from experiments).

Now, to calculate the optical conductivity, we need the knowledge of the basic block $\Phi^0_{i\varepsilon}(i\omega,\mathbf{q})$ entering Eq. (13), or, more precisely, appropriate functions analytically continued to real frequencies, $\Phi^{0RA}_{\varepsilon}(\omega,\mathbf{q})$ and $\Phi^{0RR}_{\varepsilon}(\omega,\mathbf{q})$, which in turn define $\phi^{0RA}_{\varepsilon}(\omega)$ and $\phi^{0RR}_{\varepsilon}(\omega)$ entering Eq. (22) and are defined by obvious relations similar to Eq. (13):

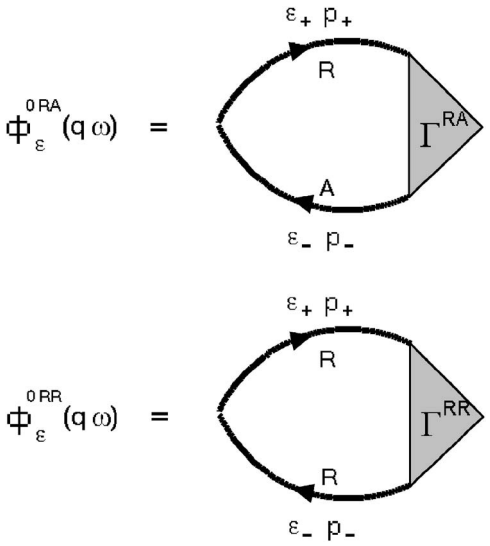

FIG. 5. Diagrammatic representation of $\Phi^{0RA}_{\varepsilon}(\omega,\mathbf{q})$.

$$\phi^{0RA}_{\varepsilon}(\omega) = \lim_{q\to 0} \frac{\Phi^{0RA}_{\varepsilon}(\omega,\mathbf{q}) - \Phi^{0RA}_{\varepsilon}(\omega,0)}{q^2}, \tag{25}$$

$$\phi^{0RR}_{\varepsilon}(\omega) = \lim_{q\to 0} \frac{\Phi^{0RR}_{\varepsilon}(\omega,\mathbf{q}) - \Phi^{0RR}_{\varepsilon}(\omega,0)}{q^2}. \tag{26}$$

By definition, we have

$$\Phi^{0RA}_{\varepsilon}(\omega,\mathbf{q}) = \sum_{\mathbf{p}} G^R(\varepsilon_+,\mathbf{p}_+)G^A(\varepsilon_-,\mathbf{p}_-)\Gamma^{RA}(\varepsilon_-,\mathbf{p}_-;\varepsilon_+,\mathbf{p}_+),$$

$$\Phi^{0RR}_{\varepsilon}(\omega,\mathbf{q}) = \sum_{\mathbf{p}} G^R(\varepsilon_+,\mathbf{p}_+)G^R(\varepsilon_-,\mathbf{p}_-)\Gamma^{RR}(\varepsilon_-,\mathbf{p}_-;\varepsilon_+,\mathbf{p}_+), \tag{27}$$

which are shown diagrammatically in Fig. 5. Here, Green's functions $G^R(\varepsilon_+,\mathbf{p}_+)$ and $G^A(\varepsilon_-,\mathbf{p}_-)$ are defined by an analytic continuation $(i\varepsilon\to\varepsilon\pm i\delta)$ of the Matsubara Green's functions (1) determined by the recurrence procedure [Eq. (23)], while vertices $\Gamma^{RA}(\varepsilon_-,\mathbf{p}_-;\varepsilon_+,\mathbf{p}_+)$ and $\Gamma^{RR}(\varepsilon_-,\mathbf{p}_-;\varepsilon_+,\mathbf{p}_+)$ containing all vertex corrections due to pseudogap fluctuations are given by the recurrence procedure, derived first (for one-dimensional case) in Ref. 22 (see also Ref. 19) and generalized for the two-dimensional problem in Ref. 23 (see also Ref. 3). The basic idea used here is that an arbitrary diagram for the vertex part can be obtained by an insertion of an "external field" line into the appropriate diagram for the self-energy.[22–24] In our model, we can limit ourselves only to diagrams with nonintersecting interaction lines with additional combinatorial factors $s(k)$ in initial interaction vertices.[3,4,21] Thus, all diagrams for the vertex part are, in fact, generated by simple ladder diagrams with addi-

tional $s(k)$ factors associated with interaction lines[22,23] (see also Ref. 19). Then we obtain the system of recurrence relations for the vertex part $\Gamma^{RA}(\varepsilon_-,\mathbf{p}_-;\varepsilon_+,\mathbf{p}_+)$, as shown by the diagrams of Fig. 6. Analytically, it has the following form,[23] where we now also included the contributions due to local (DMFT) self-energies, originating from the DMFT+$\Sigma_{\mathbf{p}}$ loop:

$$\Gamma^{RA}_{k-1}(\varepsilon_-,\mathbf{p}_-;\varepsilon_+,\mathbf{p}_+) = 1 + \Delta^2 s(k) G^A_k(\varepsilon_-,\mathbf{p}_-) G^R_k(\varepsilon_+,\mathbf{p}_+) \times \left\{ 1 + \frac{2iv_k\kappa k}{\omega - \varepsilon_k(\mathbf{p}_+) + \varepsilon_k(\mathbf{p}_-) - \Sigma^R(\varepsilon_+) + \Sigma^A(\varepsilon_-) - \Sigma^R_{k+1}(\varepsilon_+,\mathbf{p}_+) + \Sigma^A_{k+1}(\varepsilon_-,\mathbf{p}_-)} \right\} \Gamma^{RA}_k(\varepsilon_-,\mathbf{p}_-;\varepsilon_+,\mathbf{p}_+), \tag{28}$$

and

$$G^{R,A}_k(\varepsilon_\pm,\mathbf{p}_\pm) = \frac{1}{\varepsilon_\pm - \varepsilon_k(\mathbf{p}_\pm) \pm ikv_k\kappa - \Sigma^{R,A}(\varepsilon_\pm) - \Sigma^{R,A}_{k+1}(\varepsilon_\pm,\mathbf{p}_\pm)}. \tag{29}$$

The "physical" vertex $\Gamma^{RA}(\varepsilon_-,\mathbf{p}_-;\varepsilon_+,\mathbf{p}_+)$ is determined as $\Gamma^{RA}_{k=0}(\varepsilon_-,\mathbf{p}_-;\varepsilon_+,\mathbf{p}_+)$. The recurrence procedure [Eq. (28)] takes into account *all* perturbation theory diagrams for the vertex part. For $\kappa\to 0$ ($\xi\to\infty$), Eq. (28) reduces to the series studied in Ref. 24 (cf. also Ref. 3); which can be summed exactly in an analytic form. The standard "ladder" approximation in our scheme corresponds to the case of combinatorial factors $s(k)$ in Eq. (28) being equal to 1.[22]

The recurrence procedure for $\Gamma^{RR}(\varepsilon_-,\mathbf{p}_+;\varepsilon_+,\mathbf{p}_+)$ differs from Eq. (28) only by obvious replacements $A\to R$ and the whole expression in figure brackets in the right-hand side of Eq. (28) just replaced by 1:

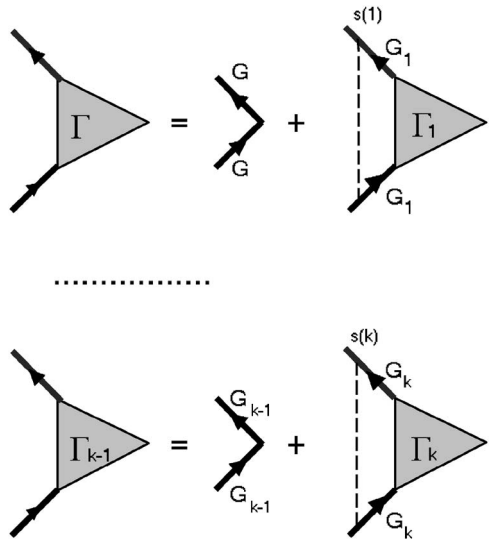

FIG. 6. Recurrence relations for the vertex part. Dashed lines denote Δ^2.

$$\Gamma^{RR}_{k-1}(\varepsilon_-,\mathbf{p}_-;\varepsilon_+,\mathbf{p}_+) = 1 + \Delta^2 s(k) G^R_k(\varepsilon_-,\mathbf{p}_-) G^R_k(\varepsilon_+,\mathbf{p}_+) \Gamma^{RR}_k(\varepsilon_-,\mathbf{p};\varepsilon_+,\mathbf{p}_+). \tag{30}$$

Note that the DMFT (Hubbard) interaction enters these equations only via local self-energies $\Sigma^{R,A}(\varepsilon_\pm)$ calculated self-consistently according to our DMFT+$\Sigma_{\mathbf{p}}$ procedure.

Equations (1), (23), (28), and (30), together with Eqs. (22), (25), and (26), provide us with the complete self-consistent procedure to calculate the optical conductivity of our model using the DMFT+$\Sigma_{\mathbf{p}}$ approach.

IV. RESULTS AND DISCUSSION

A. Generalities

In the following, we shall discuss our results for a standard one-band Hubbard model on a square lattice. The bare electronic dispersion in tight-binding approximation, with the account of the nearest- (t) and next-nearest- (t') neighbor hoppings, is given by

$$\varepsilon(\mathbf{p}) = -2t(\cos p_x a + \cos p_y a) - 4t' \cos p_x a \cos p_y a, \tag{31}$$

where a is the lattice constant. To be concrete, below we present the results for $t=0.25$ eV (more or less typical for cuprates) and $t'/t=-0.4$ (which gives Fermi surface similar to those observed in many cuprates).

For the square lattice, the bare bandwidth is $W=8t$. To study strongly correlated metallic state obtained as doped Mott insulator, we have used the value for the Hubbard interaction $U=40t$ and filling factors $n=1.0$ (half-filling) and $n=0.8$ (hole doping). For correlated metal with $W\gtrsim U$, we have taken typical values such as $U=4t$, $U=6t$, and $U=10t$ for $U\gtrsim W$. Calculations were performed for different fillings: half-filling ($n=1.0$) and for hole doping ($n=0.8,0.9$). For the typical values for Δ, we have chosen $\Delta=t$ and $\Delta=2t$ and for correlation length $\xi=2a$ and $\xi=10a$ (motivated mainly by the experimental data for cuprates[2,3]).

To solve an effective Anderson impurity problem of DMFT, we applied a reliable numerically exact method of numerical renormalization group (NRG),[25,26] which, actually,

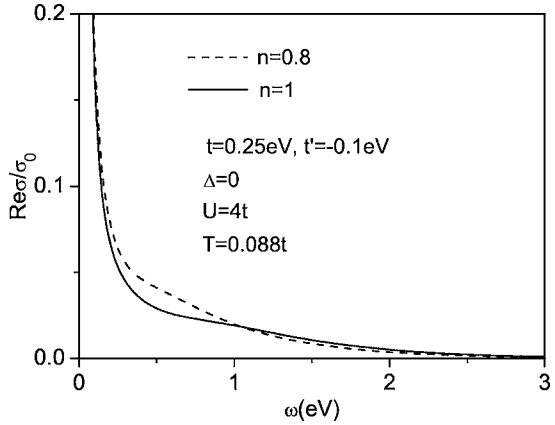

FIG. 7. Real part of the optical conductivity for correlated metal ($U=4t$, $t'=-0.4t$, and $t=0.25$ eV) in the DMFT approximation for two values of filling factor: $n=1$ and $n=0.8$. Temperature $T=0.088t$.

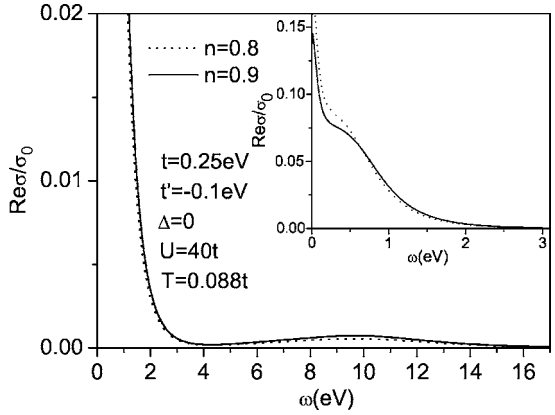

FIG. 8. Real part of the optical conductivity for doped Mott insulator ($U=40t$, $t'=-0.4t$, and $t=0.25$ eV) in the DMFT approximation. Filling factors are $n=0.8$ and $n=0.9$, and temperature $T=0.088t$. Small frequency behavior is shown in more detail in the inset.

allowed us to work with real frequencies from the very beginning, overcoming possible difficulties of performing analytical continuation numerically. Calculations were performed for two different temperatures: $T=0.088t$ and $T=0.356t$.

All necessary integrations were done directly, e.g., over the whole Brillouin zone (with the account of obvious symmetries) or wide enough frequency range. Integration momenta are made dimensionless in a natural way with the help of the lattice constant a. The conductivity is measured in units of the universal conductivity in two dimensions: $\sigma_0 = \frac{e^2}{\hbar} = 2.5 \times 10^{-4}\ \Omega^{-1}$.

B. Optical conductivity in standard DMFT

The optical conductivity was calculated for different combinations of the parameters of the model. Below, we present only a fraction of our results, which are, probably, most relevant for copper oxides. We shall start with presenting some typical results, obtained within our formalism in conventional DMFT approximation, neglecting pseudogap fluctuations, just to introduce the basic physical picture and demonstrate the effectiveness of our approach.

The characteristic feature of the strongly correlated metallic state is the coexistence of lower and upper Hubbard bands splitt by the value of $\sim U$ with a quasiparticle peak at the Fermi level.[7,8] For the case of a strongly correlated metal with $W \gtrsim U$, we observe almost no contribution from excitations to the upper Hubbard model in the optical conductivity, as can be seen in Fig. 7 [where we show the real part of conductivity Re $\sigma(\omega)$]. This contribution is almost completely masked by a typical Drude-like frequency behavior, with only slightly nonmonotonous behavior for $\omega \sim U$, which completely disappears as we increase the temperature.

The situation is different in doped Mott insulator with $U \gg W$. In Fig. 8, we clearly observe an additional maximum of optical absorption for $\omega \sim U$; however, at smaller frequencies, we again observe a typical Drude-like behavior, slightly nonmonotonous for small frequencies due to quasiparticle band formation (see the inset in Fig. 8).

These and similar results are more or less well known from the previous studies[7,8] and are quoted here only to demonstrate the consistency of our formalism and to prepare the reader for other results, showing pseudogap behavior.

C. Optical conductivity in DMFT+$\Sigma_{\mathbf{p}}$

1. Correlated metal

Let us start the discussion of the results obtained within our generalized DMFT+$\Sigma_{\mathbf{p}}$ approach for the case of $W \gtrsim U$.

In Fig. 9, we show our DMFT+$\Sigma_{\mathbf{p}}$ results for the real part of the optical conductivity for correlated metal ($U=4t$) for two values of temperature, compared with similar data without pseudogap fluctuations (pure DMFT). We clearly observe the formation of typical pseudogap (absorption) anomaly on the "shoulder" of the Drude-like peak, which is partially "filled" with the growth of temperature. This behavior is quite similar to "midinfrared feature" that is observed in the

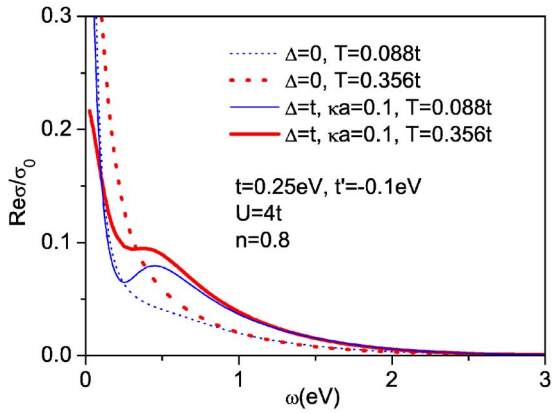

FIG. 9. (Color online) Real part of the optical conductivity for correlated metal ($U=4t$, $t'=-0.4t$, and $t=0.25$ eV) in the DMFT+$\Sigma_{\mathbf{p}}$ approximation for two different temperatures: $T=0.088t$ and $T=0.356t$. Pseudogap amplitude $\Delta=t$, correlation length $\xi=10a$, and filling factor $n=0.8$ electrons per atom.

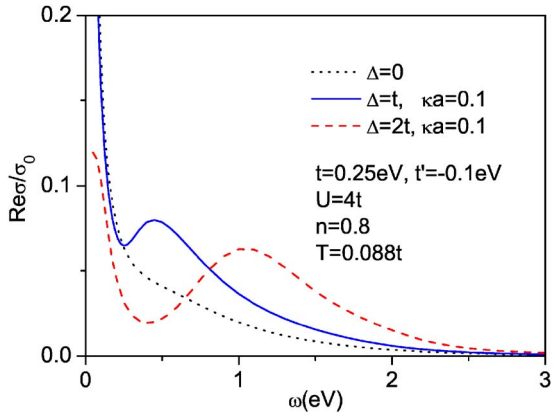

FIG. 10. (Color online) Real part of the optical conductivity for correlated metal ($U=4t$, $t'=-0.4t$, and $t=0.25$ eV) in the DMFT $+\Sigma_{\mathbf{p}}$ approximation—Δ dependence. Parameters are the same as in Fig. 9, but the data are for different values of $\Delta=0$, $\Delta=t$, and $\Delta=2t$, and temperature $T=0.088t$.

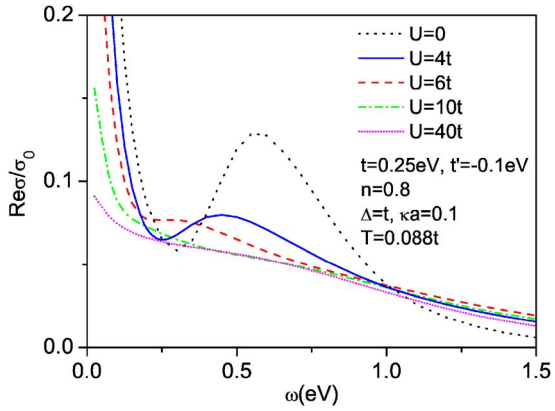

FIG. 12. (Color online) Real part of the optical conductivity for correlated metal in the DMFT+$\Sigma_{\mathbf{p}}$ approximation—U dependence. Parameters are the same as in Fig. 9, but the data are for different values of U: $U=0$, $U=4t$, $U=6t$, $U=10t$, and $U=40t$. Temperature $T=0.088t$.

optical conductivity of cuprate superconductors.[27,28] In Fig. 10, we show the behavior of Re $\sigma(\omega)$ for different values of the pseudogap amplitude Δ. We see that the pseudogap anomaly naturally grows with the growth of Δ. Figure 11 illustrates the dependence of Re $\sigma(\omega)$ on the correlation length of pseudogap (AFM, SDW) fluctuations. Again, we observe the natural behavior—pseudogap anomaly is filled for shorter correlation lengths, i.e., as fluctuations become more short ranged. At last, in Fig. 12, we demonstrate the dependence of the pseudogap anomaly in the optical conductivity on the correlation strength, i.e., on the Hubbard interaction U. It is seen that the frequency range, where pseudogap anomaly is observed, becomes narrower as the correlation strength grows. This correlates with the general narrowing of the pseudogap anomaly and spectral densities with the growth of correlations, as observed in our previous work.[15,16] For large values of U, the pseudogap anomaly is practically suppressed. This is the main qualitative difference

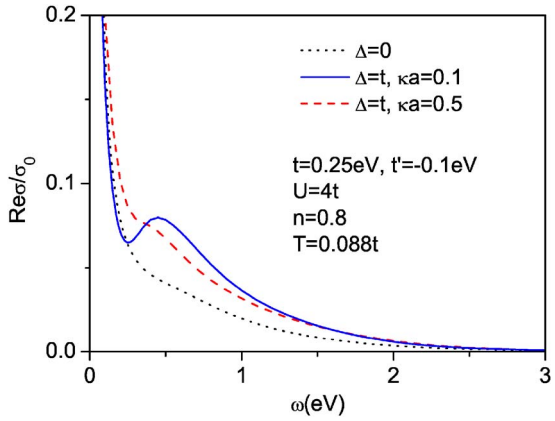

FIG. 11. (Color online) Real part of the optical conductivity for correlated metal ($U=4t$, $t'=-0.4t$, and $t=0.25$ eV) in the DMFT $+\Sigma_{\mathbf{p}}$ approximation—dependence on the correlation length. Parameters are the same as in Fig. 9, but in the data are for different values of the inverse correlation length $\kappa=\xi^{-1}$: $\kappa a=0.1$ and $\kappa a=0.5$, and temperature $T=0.088t$.

of the results of the present approach compared to our earlier work[23] on the optical conductivity in the pseudogap state. Comparing the data of the present work for $U=0$ with similar data of Ref. 23, it should be noted that in this earlier work, we have performed calculations of dynamic conductivity only for $T=0$ and used simplified expressions, neglecting *RR*- and *AA*-loop contributions to conductivity, as well as small frequency expansion,[18] just to speed up the calculations. These simplifications lead to some quantitative differences with the results of the present work, where all calculations are done exactly using the general expression (22), though qualitatively the frequency behavior of conductivity is the same.

2. Doped Mott insulator

Now, we shall discuss our results for the case of doped Mott insulator with $U \gg W$. This case has no direct relevance to copper oxides, but is interesting from the general point of view and we present some of our results.

The real part of the optical conductivity for the case of $U=40t$ is shown in Figs. 13 and 14.

In Fig. 13, we show Re $\sigma(\omega)$ several values of the pseudogap amplitude Δ for the doped Mott insulator in the DMFT+$\Sigma_{\mathbf{p}}$ approach. Obviously enough, pseudogap fluctuations lead to significant changes of the optical conductivity only for relatively small frequencies of the order of Δ, while for high frequencies (e.g., of the order of U, where the upper Hubbard band contributes), we do not observe pseudogap effects (see the inset in Fig. 13). For small frequencies, we observe pseudogap suppression of the Drude-like peak, with only a shallow anomaly for $\omega \sim \Delta$, which just disappears for smaller values of Δ or shorter correlation lengths.

In Fig. 14, we show similar data for the special case of $t'=0$ and $n=1$, i.e., at half-filling (Mott insulator) for different values of the inverse correlation length $\kappa=\xi^{-1}$. The conductivity at small frequencies is determined only by thermal excitations, and pseudogap fluctuations suppress it significantly. Shorter correlation lengths obviously lead to larger values of conductivity at small frequencies. Transitions to the

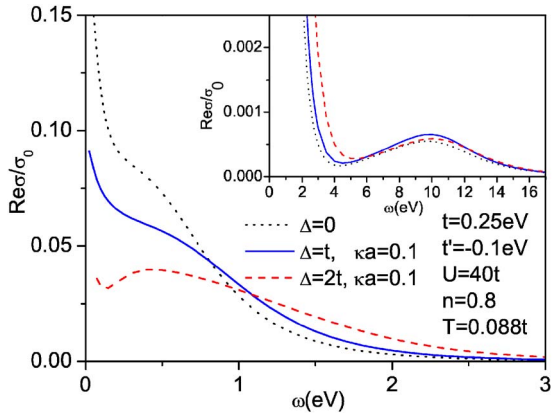

FIG. 13. (Color online) Real part of the optical conductivity for doped Mott insulator ($U=40t$, $t'=-0.4t$, and $t=0.25$ eV) in the DMFT+$\Sigma_{\mathbf{p}}$ approximation for different values of $\Delta=0$, $\Delta=t$, and $\Delta=2t$, and temperature $T=0.088t$. Correlation length $\xi=10a$, and filling factor $n=0.8$. Inset: conductivity in a wide frequency interval, including transitions to the upper Hubbard band.

upper Hubbard band are not affected by these fluctuations at all.

V. CONCLUSION

The present work is the direct continuation of our previous work,[14–16] where we have proposed a generalized DMFT+$\Sigma_{\mathbf{p}}$ approach, which is meant to take into account the important effects of nonlocal correlations (in principle, of any type) in addition to the (essentially exact) treatment of local dynamical correlations by DMFT. Here, we used a generalized DMFT+$\Sigma_{\mathbf{p}}$ approach to calculate the dynamic (optical) conductivity of the two-dimensional Hubbard model with pseudogap fluctuations. Our results demonstrate that pseudogap anomalies observed in optical conductivity of copper oxides can, in principle, be explained by this model. The main advantage in comparison to the previous work[23] is our ability now to study the role of strong electronic correlations, which are decisive in the formation of electronic structure of systems such as copper oxides. In fact, we have demonstrated an important suppression of pseudogap anomaly in optical conductivity with the growth of correlation strength.

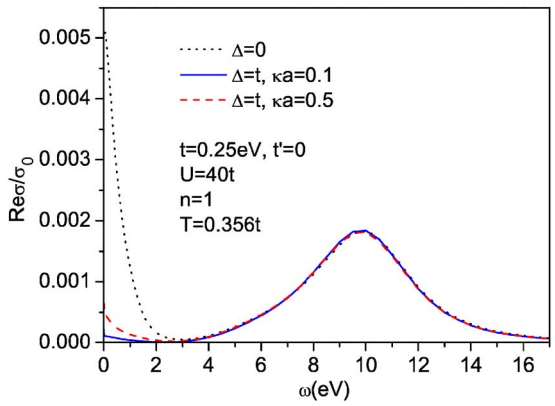

FIG. 14. (Color online) Real part of the optical conductivity for doped Mott insulator ($U=40t$, $t=0.25$ eV, and $t'=0$) in the DMFT+$\Sigma_{\mathbf{p}}$ approximation for different values of the inverse correlation length $\kappa=\xi^{-1}$: $\kappa a=0.1$ and $\kappa a=0.5$, temperature $T=0.356t$, and filling $n=1$.

As we already noted in Ref. 15, qualitatively similar results on pseudogap formation in single-particle characteristics for the two-dimensional Hubbard model were also obtained within cluster extensions of DMFT.[12,13] However, these methods have generic restrictions concerning the size of the cluster and up to now have not been not widely applied to calculations of two-particle properties, such as general response functions, and, in particular, to calculations of the dynamic (optical) conductivity.

Our approach is free of these limitations, though at the price of introduction of additional (semi)phenomenological parameters (correlation length ξ and pseudogap amplitude Δ). It is much less time consuming; thus its advantage for the calculations of two-particle response functions is obvious. It also opens the possibility of systematic comparison of different types of nonlocal fluctuations and their effects on electronic properties, providing a more intuitive way to analyze experiments or theoretical data obtained within more advanced schemes. Again, note that, in principle, both ξ and Δ can be calculated from the original model.[15] Our scheme works for any Coulomb interaction strength U, pseudogap strength Δ, correlation length ξ, filling n, and bare electron dispersion $\varepsilon(\mathbf{k})$.

The present formalism can be easily generalized in the framework of our recently proposed LDA+DMFT+$\Sigma_{\mathbf{p}}$ approach, which will allow us to perform calculations of pseudogap anomalies of the optical conductivity for realistic models. It can also be easily generalized to orbital degrees of freedom, phonons, impurities, etc.

ACKNOWLEDGMENTS

We are grateful to Th. Pruschke for providing us with his effective NRG code. This work was supported in part by RFBR Grants No. 05-02-16301 (M.V.S., E.Z.K., and I.A.N.), No. 05-02-17244 (I.A.N.), No. 06-02-90537 (I.A.N.), by the joint UrO-SO project (E.Z.K. and I.A.N.), and by the programs of the Presidium of the Russian Academy of Sciences (RAS) "Quantum macrophysics" and of the Division of Physical Sciences of the RAS "Strongly correlated electrons in semiconductors, metals, superconductors, and magnetic materials." I.A.N. acknowledges the support from the Dynasty Foundation and International Center for Fundamental Physics in Moscow program for young scientists and also from the grant of the President of the Russian Federation for young Ph.D. MK-2118.2005.02.

VI. APPENDIX: WARD IDENTITIES

In this appendix, we present the derivation of Ward identities used in the main text. Let us start with the general expression for the variation of the electron self-energy due to an arbitrary variation of the complete Green's function, which is valid for any interacting Fermi system:[29]

$$\Delta\Sigma_p = \sum_{p'} U_{pp'}(q)\Delta G_{p'}, \tag{A1}$$

where $U_{pp'}(q)$ is an irreducible vertex in particle-hole channel, and we use four-dimensional notations $p=(i\varepsilon,\mathbf{p})$, $q=(i\omega,\mathbf{q})$, etc. In the following, we take

$$\Delta\Sigma_p = \Sigma_+ - \Sigma_- \equiv \Sigma(i\varepsilon_+,\mathbf{p}_+) - \Sigma(i\varepsilon_-,\mathbf{p}_-), \tag{A2}$$

and (in the same notations)

$$\Delta G_p = G_+ - G_- = (G_+G_-)_p\left[\Delta\Sigma_p - \Delta(G_0^{-1})_p\right], \tag{A3}$$

where $\Delta(G_0^{-1})_p = G_{0+}^{-1} - G_{0-}^{-1}$, and the last expression was obtained using the standard Dyson equation.

Note the similarity of Eq. (A1) to the Ward identity for noninteracting electrons in the impure system derived in Ref. 18.

Now, substituting the last expression in Eq. (A3), we get

$$\Delta\Sigma_p = \sum_{p'} U_{pp'}(q)(G_+G_-)_{p'}\left[\Delta\Sigma_{p'} - \Delta(G_0^{-1})_{p'}\right]. \tag{A4}$$

Iterating this equation, we obtain

$$\Delta\Sigma_p = \sum_{p'} U_{pp'}(G_+G_-)_{p'}[-\Delta(G_0^{-1})_{p'}] + \sum_{p''p'} U_{pp''}(G_+G_-)_{p''}U_{p''p'}(G_+G_-)_{p'}[-\Delta(G_0^{-1})_{p'}] + \cdots. \tag{A5}$$

Multiplying both sides of Eq. (A5) by $(G_+G_-)_p$ and adding

$$\sum_{p'} (G_+G_-)_p\delta_{pp'}[-\Delta(G_0^{-1})_{p'}] = (G_+G_-)_p[-\Delta(G_0^{-1})_p],$$

we have

$$\begin{aligned}(G_+G_-)_p&\left[\Delta\Sigma_p - \Delta(G_0^{-1})_p\right] \\ &= \sum_{p'}\Bigg[(G_+G_-)_p\delta_{pp'} + (G_+G_-)_pU_{pp'}(G_+G_-)_{p'} + (G_+G_-)_p \\ &\quad\times\sum_{p''} U_{pp''}(G_+G_-)_{p''}U_{p''p'}(G_+G_-)_{p'} + \cdots\Bigg][-\Delta(G_0^{-1})] \\ &= \sum_p \Phi_{pp'}(q)[-\Delta(G_0^{-1})_{p'}],\end{aligned} \tag{A6}$$

where $\Phi_{pp'}(q)$ is the complete two-particle Green's function determined by the following Bethe-Salpeter equation:[29]

$$\Phi_{pp'}(q) = (G_+G_-)_p\delta_{pp'} + (G_+G_-)_p\sum_{p'} U_{pp'}\Phi_{pp'}(q). \tag{A7}$$

Finally, we obtain

$$\Delta G_p = \sum_{p'} \Phi_{pp'}(q)[-\Delta(G_0^{-1})_{p'}], \tag{A8}$$

which is the general form of our Ward identity.

Summing both sides of Eq. (A8) over $\mathbf{p}$ and taking $\mathbf{q}=0$, we obtain the identity (16) used above. Similarly, taking the bare Green's function (17), we obtain Eq. (18).

[1] T. Timusk and B. Statt, Rep. Prog. Phys. **62**, 61 (1999).
[2] M. V. Sadovskii, Usp. Fiz. Nauk **171**, 539 (2001) [Phys. Usp. **44**, 515 (2001)].
[3] J. Schmalian, D. Pines, and B. Stojkovič, Phys. Rev. Lett. **80**, 3839 (1998); Phys. Rev. B **60**, 667 (1999).
[4] E. Z. Kuchinskii and M. V. Sadovskii, Zh. Eksp. Teor. Fiz. **115**, 1765 (1999) [JETP **88**, 347 (1999)].
[5] W. Metzner and D. Vollhardt, Phys. Rev. Lett. **62**, 324 (1989).
[6] D. Vollhardt, in *Correlated Electron Systems*, edited by V. J. Emery (World Scientific, Singapore, 1993), p. 57.
[7] Th. Pruschke, M. Jarrell, and J. K. Freericks, Adv. Phys. **44**, 187 (1995).
[8] A. Georges, G. Kotliar, W. Krauth, and M. J. Rozenberg, Rev. Mod. Phys. **68**, 13 (1996).
[9] G. Kotliar and D. Vollhardt, Phys. Today **57**(3), 53 (2004).
[10] Q. Si and J. L. Smith, Phys. Rev. Lett. **77**, 3391 (1996).
[11] EDMFT approach to pseudogap formation can be found in K. Haule, A. Rosch, J. Kroha, and P. Wölfle, Phys. Rev. Lett. **89**, 236402 (2002); Phys. Rev. B **68**, 155119 (2003).
[12] Th. Maier, M. Jarrell, Th. Pruschke, and M. Hettler, Rev. Mod. Phys. **77**, 1027 (2005).
[13] G. Kotliar, S. Y. Savrasov, G. Palsson, and G. Biroli, Phys. Rev. Lett. **87**, 186401 (2001); M. Capone, M. Civelli, S. S. Kancharla, C. Castellani, and G. Kotliar, Phys. Rev. B **69**, 195105 (2004).
[14] E. Z. Kuchinskii, I. A. Nekrasov, and M. V. Sadovskii, Pis'ma Zh. Eksp. Teor. Fiz. **82**, 217 (2005) [JETP Lett. **82**, 198 (2005)].
[15] M. V. Sadovskii, I. A. Nekrasov, E. Z. Kuchinskii, Th. Pruschke, and V. I. Anisimov, Phys. Rev. B **72**, 155105 (2005).
[16] E. Z. Kuchinskii, I. A. Nekrasov, and M. V. Sadovskii, Fiz. Nizk. Temp. **32**, 528 (2006) [Low Temp. Phys. **32**, 398 (2006)].
[17] E. Z. Kuchinskii, I. A. Nekrasov, Z. V. Pchelkina, and M. V. Sadovskii, cond-mat/0606651 (to be published).
[18] D. Vollhardt and P. Wölfle, Phys. Rev. B **22**, 4666 (1980).
[19] M. V. Sadovskii, *Diagrammatics* (World Scientific, Singapore, 2006).
[20] V. Janiš, J. Kolorenč, and V. Špička, Eur. Phys. J. B **35**, 77 (2003).
[21] M. V. Sadovskii, Zh. Eksp. Teor. Fiz. **77**, 2070 (1979) [Sov. Phys. JETP **50**, 989 (1979)].
[22] M. V. Sadovskii and A. A. Timofeev, J. Mosc. Phys. Soc. **1**, 391 (1991).
[23] M. V. Sadovskii and N. A. Strigina, Zh. Eksp. Teor. Fiz. **122**, 610 (2002) [JETP **95**, 526 (2002)].
[24] M. V. Sadovskii, Zh. Eksp. Teor. Fiz. **66**, 1720 (1974) [Sov. Phys. JETP **39**, 845 (1974)].
[25] K. G. Wilson, Rev. Mod. Phys. **47**, 773 (1975); H. R. Krishnamurthy, J. W. Wilkins, and K. G. Wilson, Phys. Rev. B **21**, 1003

(1980); **21**, 1044 (1980); A. C. Hewson, *The Kondo Problem to Heavy Fermions* (Cambridge University Press, Cambridge, 1993).

[26] R. Bulla, A. C. Hewson, and Th. Pruschke, J. Phys.: Condens. Matter **10**, 8365 (1998); R. Bulla, Phys. Rev. Lett. **83**, 136 (1999).

[27] D. N. Basov and T. Timusk, Rev. Mod. Phys. **77**, 721 (2005).

[28] J. Hwang, T. Timusk, and G. D. Gu, cond-mat/0607653 (to be published).

[29] A. B. Migdal, *Theory of Finite Fermi Systems and Applications to Atomic Nuclei* (Interscience Publishers, New York, 1967).